



This is a repository copy of *Toughening mechanism of carbon fibre reinforced polymer laminates containing inkjet printed poly(methyl methacrylate) microphases*.

White Rose Research Online URL for this paper:

<https://eprints.whiterose.ac.uk/119787/>

Version: Accepted Version

Article:

Zhang, Y., Stringer, J., Hodzic, A. et al. (1 more author) (2018) Toughening mechanism of carbon fibre reinforced polymer laminates containing inkjet printed poly(methyl methacrylate) microphases. *Journal of Composite Materials*, 52 (11). pp. 1567-1576. ISSN 0021-9983

<https://doi.org/10.1177/0021998317727133>

Reuse

Items deposited in White Rose Research Online are protected by copyright, with all rights reserved unless indicated otherwise. They may be downloaded and/or printed for private study, or other acts as permitted by national copyright laws. The publisher or other rights holders may allow further reproduction and re-use of the full text version. This is indicated by the licence information on the White Rose Research Online record for the item.

Takedown

If you consider content in White Rose Research Online to be in breach of UK law, please notify us by emailing eprints@whiterose.ac.uk including the URL of the record and the reason for the withdrawal request.



eprints@whiterose.ac.uk
<https://eprints.whiterose.ac.uk/>

**Toughening Mechanism of Carbon Fibre Reinforced Polymer
Laminates Containing Inkjet Printed Poly(methyl methacrylate)
Microphases**

Yi Zhang^{1,*}, Jonathan Stringer², Alma Hodzic³ and Patrick J. Smith^{1,*}

¹ Composite Systems Innovation Centre (CSIC), Department of Mechanical Engineering, The University of Sheffield, Sheffield, UK

² Department of Mechanical Engineering, University of Auckland, Auckland, New Zealand

³ Revaluetechn Ltd., Birmingham, UK

*Corresponding author: Dr Yi Zhang, Dr Patrick J. Smith

Email: yi.zhang@sheffield.ac.uk, patrick.smith@sheffield.ac.uk

Abstract

It has previously been demonstrated that inkjet printed thermoplastic microphases are capable of producing a significant increase in mode I interlaminar fracture toughness (G_{Ic}) in carbon fibre reinforced polymer (CFRP) with no significant reduction in other mechanical properties or increase in parasitic weight. In this work, the evolution of the microphase structure during processing and how this is influenced by the chosen printing parameters was investigated. Samples were prepared that enabled monitoring of the microphases during all steps of fabrication, with the thermoplastic polymer found to form a discrete spherical shape due to surface energy minimisation. Based upon the

morphology and properties of the thermoplastic microphases, it was hypothesised that the increased toughness was due to a combination of crack deflection and plastic deformation of the microphases. Samples were produced for the double cantilever beam fracture toughness testing using the same printing conditions, and both G_{Ic} values and scanning electron microscopy (SEM) of the fracture surface supported the proposed hypothesis. The feasibility of selective toughening is also demonstrated, which presents potential to tailor the mechanical properties of the CFRP spatially.

Keywords: toughening mechanism, fracture toughness, inkjet printing, CFRP, PMMA

1. Introduction

While carbon fibre reinforced polymer (CFRP) laminates have made a remarkable breakthrough in a range of industries on account of their favourable mechanical properties such as high stiffness-weight and strength-weight ratios, a major concern of using this material is its susceptibility to delamination. This is because the brittle nature of epoxy is prone to develop microcracks when subjected to stress, and these microcracks tend to develop between laminate plies due to the laminated materials lacking reinforcement in the through thickness direction ¹. This can eventually lead to delamination, which is a typical failure mode commonly seen in the laminated CFRP. To improve the delamination resistance of CFRP, interleaving of high toughness materials between laminate plies has been demonstrated as an effective method to improve the interlaminar fracture toughness

²⁻⁷. However, a major trade-off associated with this toughening method is the parasitic weight penalty, which compromises the high stiffness-weight and strength-weight ratios of CFRP laminates. Moreover, interleaving is directly correlated with the reduction in the interlaminar shear properties and fibre volume fraction ⁴. Therefore, minimising weight gain due to the application of toughening material has been of great interest.

Drop-on-demand inkjet printing is a direct write additive manufacturing method which can generate uniform droplets in picolitre (pL) volume scale and precisely dispense those droplets directly into pre-designed patterns without masks ⁸⁻¹⁰. Our previous studies show that the mode I interlaminar fracture toughness (G_{Ic}) of CFRP laminates with inkjet printed poly(methyl methacrylate) (PMMA) microphases between laminate plies was noticeably improved compared to the baseline (i.e. without printed PMMA) without decrease in interlaminar shear strength (ILSS). By depositing approximately 0.05 vol.% of PMMA microphases between CFRP laminate plies, the G_{Ic} was improved by approximately 40% compared to the baseline, indicating that inkjet printing has the achievable potential to be used as means of introducing toughening material without introducing excessive weight which is detrimental to other material properties ¹¹⁻¹⁴.

In order to better understand the toughening mechanism, the evolution of how the printed PMMA goes from the printed pattern to the toughening structure during CFRP laminate fabrication and curing is investigated in this paper. The investigation was performed by

constructing a replica system of the CFRP that is optically transparent, which enables the monitoring of the microphase structure at various stages of CFRP laminate fabrication. Knowledge of the structure in the as-produced CFRP was then correlated with mechanical properties and fractography of CFRP laminate test samples to elucidate the toughening mechanism. Better understanding of the toughening mechanism will then allow more specific optimisation of the printing parameters to a given application, with a potential for spatially-targeted toughening in the desired areas of CFRP laminate.

2. Experimental

2.1 Solution preparation for inkjet printing

PMMA (M_w ~ 15 kDa) was dissolved in N, N-dimethylformamide (DMF) to form 10 wt.% and 20 wt.% PMMA solutions respectively for printing. All chemicals were purchased from Sigma Aldrich (Sigma-Aldrich Co. Ltd., UK) and used as received. Ultrasonic agitation was used to aid the dissolution of PMMA in DMF.

2.2 Preparation of neat resin coated glass slides with printed PMMA deposits

Epoxy resin (CYCOM[®] 977-20 RTM resin, Cytec Engineered Materials Ltd., UK) was used to coat microscope glass slides for investigating the morphology of printed PMMA deposits embedded in epoxy resin before and after the heating cycle. All glass slides were cleaned using 2% Micro-90 and dried before coating. This epoxy resin is formulated as the resin transfer moulding version of Cytec's CYCOM[®] 977-2 toughened epoxy prepreg

resin. CYCOM[®] 977-20 resin was defrosted the day before use. Cleaned microscope glass slides were coated with a thin layer (approximately 50 μm) of the clear honey-like resin at room temperature. A pre-heat procedure was conducted to partially cure the resin to decrease its mobility on the glass slides and to be more representative of the resin typically found in uncured pre-preg. This pre-heat procedure consisted of heating the coated glass slide to 120°C for 2 hours.

PMMA solutions were printed into different patterns (i.e. hexagonal array, films and lines) onto the partially cured epoxy coated glass slides. All printed glass slides were left to dry for 24 hours at room temperature before covering with another partially cured epoxy coated glass slide for the subsequent heating. These “sandwiched” samples were then heated up to 160°C for 30 minutes with an applied pressure (5 kPa) to ensure the contact of the top and bottom glass slides of the “sandwich” samples, then cooling down to room temperature for microscopy analysis. Fig. 1 schematically shows the preparation of the “sandwich” samples.

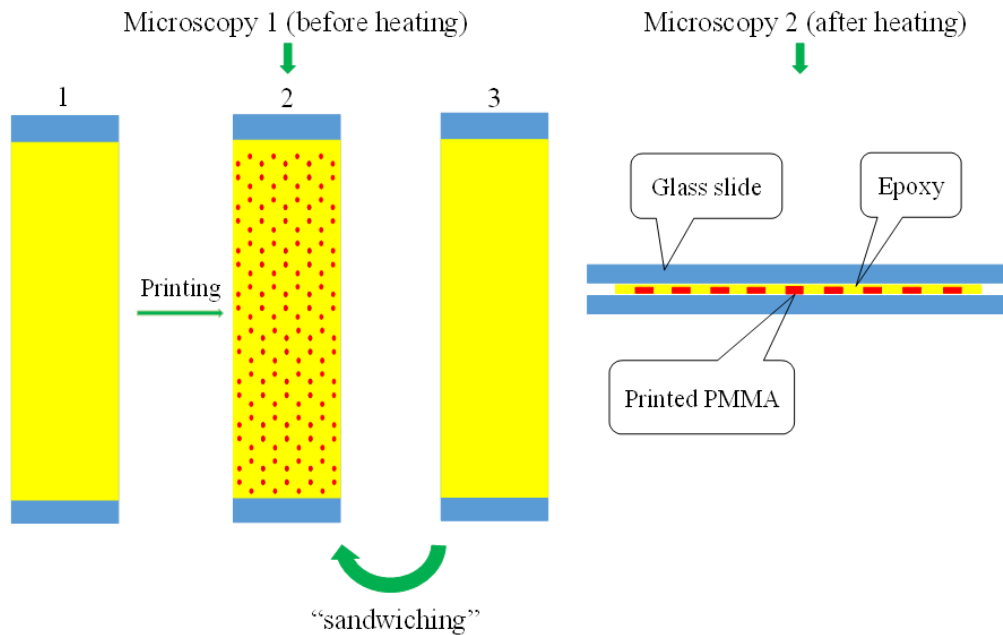


Fig. 1. A schematic of the preparation of “sandwiched” sample with inkjet printed PMMA deposits.

2.3 Fabrication of CFRP laminates

Unidirectional CFRP prepreg tape (CYCOM[®] 977-2-35-12KHTS-268-300, Cytec Engineered Materials Ltd., UK) was used to fabricate CFRP laminates. A non-stick polytetrafluoroethylene (PTFE) film was inserted at the mid-thickness ply of double cantilever beam (DCB) panel to simulate an initial crack. A customised autoclave (Premier Autoclaves Ltd., UK) was used to consolidate the laid-up laminates. . The program used for curing the parent laminates is shown in Fig. 2. The DCB samples were

cut from the parent laminates into $140 \pm 1 \text{ mm} \times 20 \pm 0.5 \text{ mm}$ strips in accordance with the DCB test standard ¹⁵. The thickness of the samples was $3.2 \pm 0.1 \text{ mm}$.

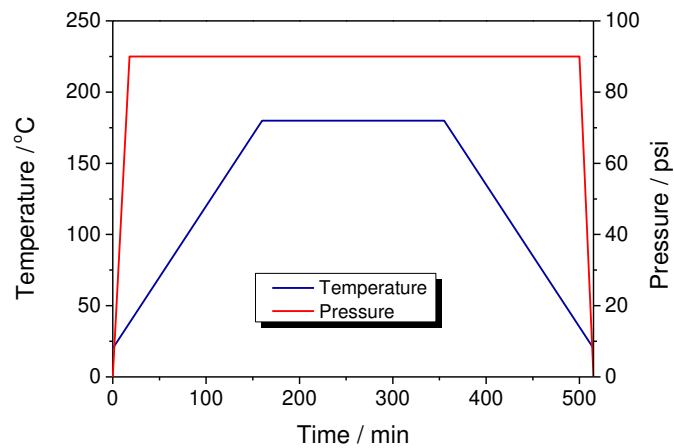


Fig. 2. Program used for consolidating CFRP laminates.

Four different patterns (Fig. 3) were designed to evaluate the pattern shape effect on the G_{Ic} of the inkjet printed CFRP laminates. The four patterns had the same amount of toughening material per unit area.

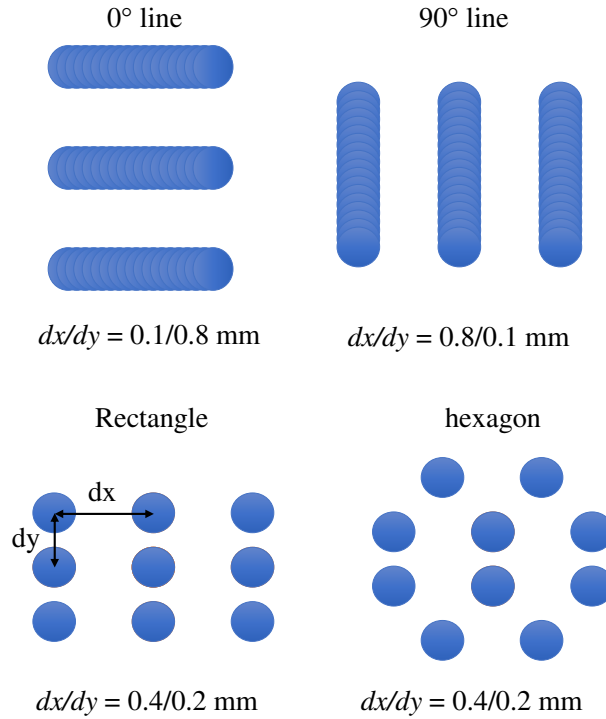


Fig. 3. Four patterns with the same amount of toughening material per unit area, where dx means the spacing between printed dots in the x -axis, and dy the spacing in y -axis.

In order to verify the effect of selective printing, 10 wt.% PMMA solution was used to prepare two different sets of DCB samples as shown in Fig. 4. For the type A sample, the second half of the test area was printed with PMMA using the hexagon pattern. For the type B samples, the first half of the test area was printed with the hexagonal PMMA pattern, the remaining half was left with no printing. Unlike the previous experiments, where the difference in G_{Ic} of printed and unprinted laminates was between different

samples, in this set of experiment, the difference was generated within one sample. Therefore, G_{Ic} values were expected to change within a single G_{Ic} -Delamination curve.

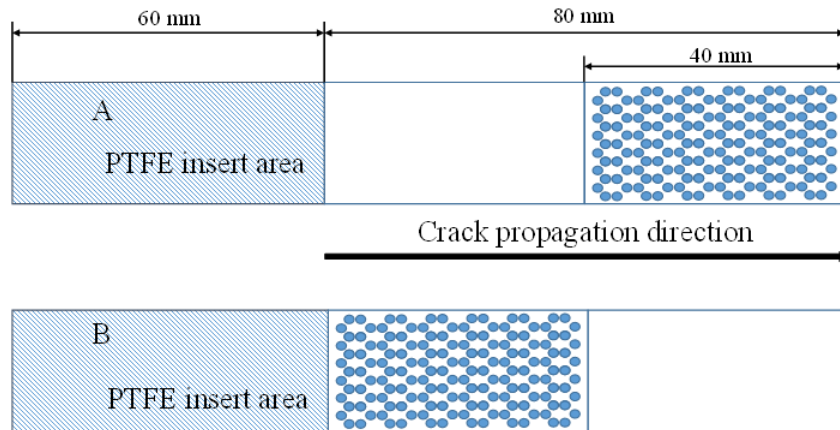


Fig. 4. Two types of DCB samples. In sample A, the crack propagates into a non-printed zone then a printed zone. In samples B, the crack front encounters a printed region first then a non-printed zone.

2.4 Test procedures

A desktop universal tester (TA500 Texture Analyser, Lloyd Instruments, UK) equipped with a 500N load cell was used to conduct the DCB test in tension mode at room temperature. The speed of crosshead was 5 mm/min. The test samples were first pre-cracked using a mode I opening load to avoid any resin rich pockets on the front of the created crack and generate a sharp crack tip for subsequent test. A high definition camcorder (HC-X920M Panasonic, Japan) was used to record the DCB test for determining the delamination length for data reduction.

3. Results and Discussion

3.1 Microphase morphology evolution

Optical microscopy images of the epoxy coated glass slides with printed PMMA deposits showed that the printed PMMA deposits formed spherical particles after the heating cycle as shown in Fig. 5(b, d and f). This would be the expected morphology formed between two immiscible and mobile phases, and is due to minimisation of surface energy. This was shown in Gomez's and Ritzenthaler's work where curing blends which contained epoxy, hardener and PMMA at a high temperature, created phase separation: blends formed discrete small particles^{16, 17}. Similarly, when curing PMMA printed epoxy resin at a high temperature, spherical particles formed, where the particles could be PMMA domains containing other additions such as hardener. For simplicity, 'PMMA particles' is used to represent these PMMA domains in the following discussion.

If the observed morphology is driven by surface energy minimisation, it would be expected that not only are the PMMA phases spherical, they are also of a size that corresponds to the amount of PMMA deposited in that location. Due to the highly repeatable nature of droplet generation in inkjet printing, it is reasonable to assume that each droplet is of the same volume, with this volume dictated by the diameter of the orifice through which a droplet is ejected. Due to surface energy minimisation, it is also reasonable to assume that the droplet is spherical. This means that each droplet deposited

can be assumed to have the same volume; with that volume equal to a sphere of diameter equal to the orifice diameter. In this work, a 60 μm diameter orifice was used, which results in droplets of 113 pL. To calculate the equivalent volume of PMMA in each droplet, the droplet volume was then further multiplied by the volume fraction of polymer within the ink, with the volume fraction being equal to the weight fraction multiplied by the density ratio of polymer and solvent (for PMMA and DMF, this is $1180/944=1.25$). For the 10 wt.% PMMA ink, this results in a deposited PMMA volume per drop of 14.12 pL, and for the 20 wt.% PMMA ink a volume of 28.25 pL.

It is hypothesised that during the heating cycle, the immiscible PMMA and epoxy phases will undergo a minimisation of surface energy, resulting in spherical PMMA particles embedded within the epoxy matrix. The diameter of these particles should be dictated by the volume of PMMA deposited at a given location, as calculated above. Assuming that the formed particles are spherical, it is possible to calculate a corresponding sphere diameter from these volumes, with a single printed droplet of 10 wt.% PMMA ink forming a spherical PMMA particle of 30.0 μm diameter and for a 20 wt.% PMMA ink droplet it is 37.8 μm diameter. For multiple droplets a similar calculation can be performed, but with the corresponding multiple of single droplet volume used.

The measured diameter of the 10 wt.% and 20 wt.% PMMA phases were $33.7 \pm 2.1\mu\text{m}$ and $36.8 \pm 2.0 \mu\text{m}$ respectively. These measurements are in reasonable agreement with

the diameters calculated above, considering the number of assumptions made in the calculation. Furthermore, measurements of the spherical particle formed from two droplets of 10 wt.% PMMA ink showed a diameter of $36.4 \pm 1.1 \mu\text{m}$, which correlates very well with the 20 wt.% PMMA results. This is to be expected as the deposited volume of PMMA in both of the aforementioned cases should be identical.

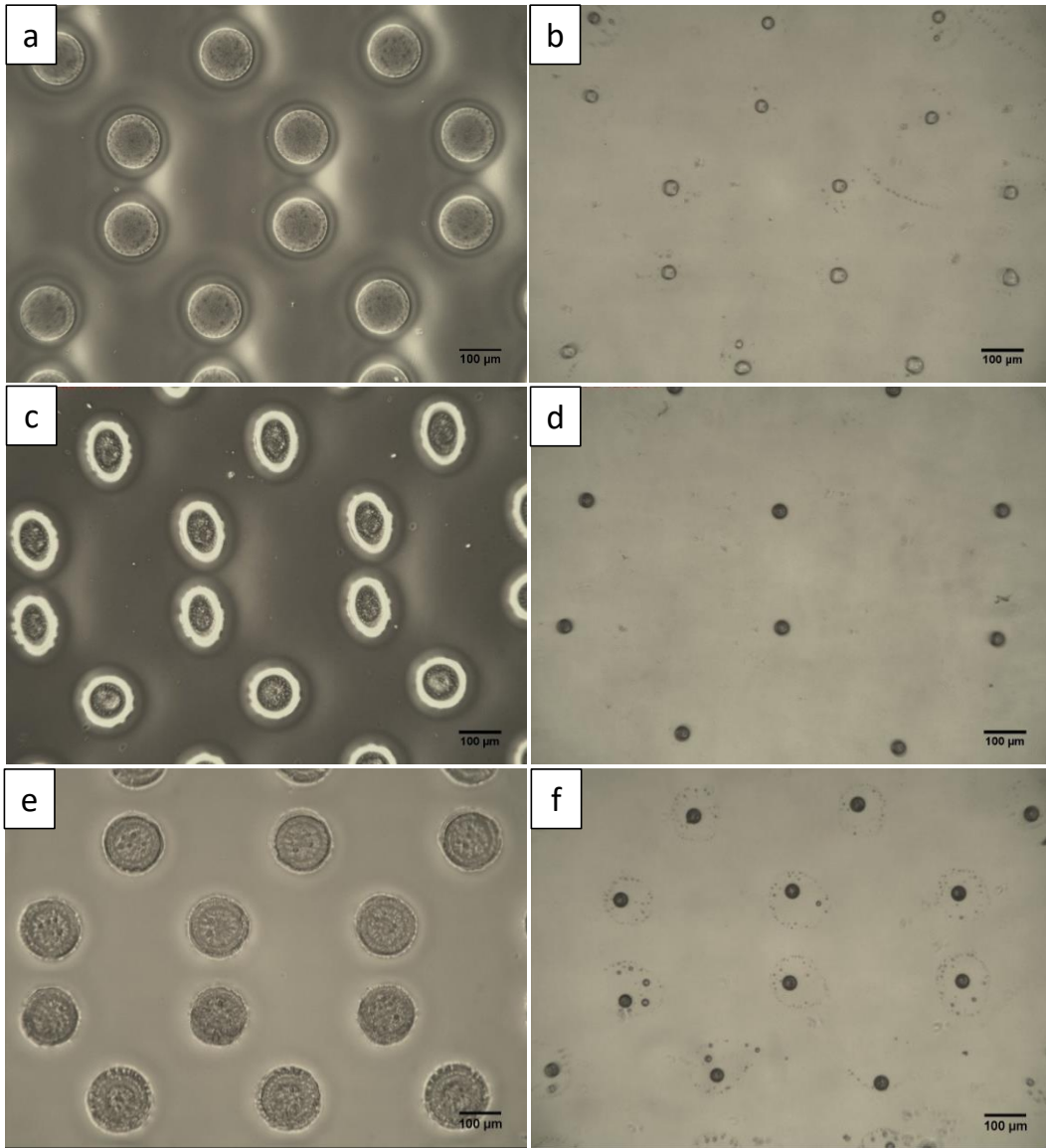


Fig. 5. The morphology evolution of PMMA discrete deposits. a, c) single printed hexagon pattern using 10 wt.% PMMA and 20 wt.% PMMA solution respectively before heating; e) double-printed hexagon pattern using 10 wt.% PMMA solution before heating; b, d, f) PMMA particles formed after heating.

Inkjet printing has the capability of depositing picolitre volume droplets, and printing a variety of patterns including continuous features such as film and lines. It is of interest to investigate the morphology evolution of these continuous phases, both lines and films, in addition to mechanical tests. As can be seen in Fig. 6(a, b), the printed PMMA thin film broke down into randomly distributed spherical particles with a wide range of diameters after heating. Fig. 6(d) shows that the printed lines also broke down into unevenly sized particles, but these particles are still partially lined up. These results suggested that the printed continuous phase of PMMA cannot be retained after curing. In the case of discrete dot patterns, the amount of PMMA at each printed position was about the same, therefore, the size of formed PMMA particles after heating was about the same with a small variation. However, the size of PMMA particles formed from a continuous phase was not controllable as observed, which may give rise to localised variations of toughening agent.

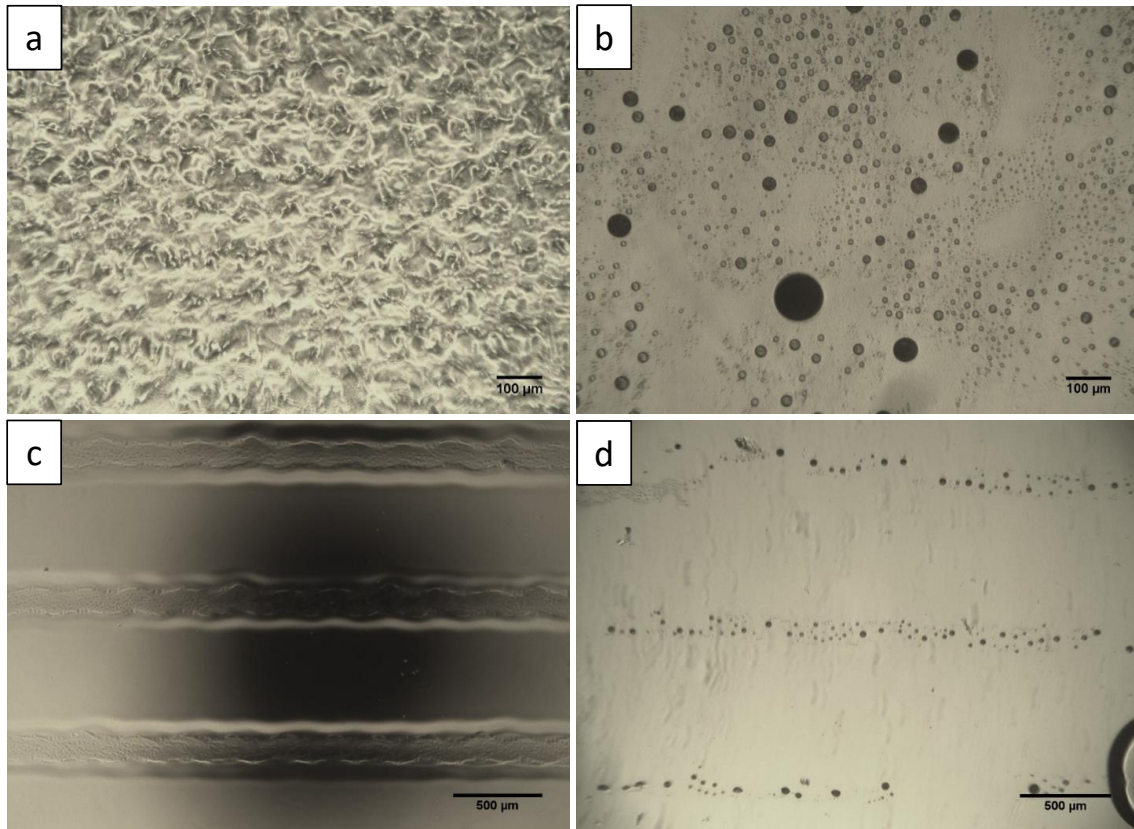


Fig. 6. The morphology evolution of PMMA continuous phases. a) film and c) lines before heating; b, d) after heating.

3.2 Fractographic analysis

The SEM images of fracture surfaces of DCB samples shown in Fig. 7 agree with the observed morphology evolution of PMMA: the printed PMMA deposits formed spherical particles after curing. Because of the complex morphology of CFRP laminates, and the severe damage done to the test surfaces, the discrete dot patterns could not be identified, however scattered PMMA particles can be spotted as shown in Fig. 7(c). The PMMA

particles formed from the printed lines are more easily spotted due to a relatively high distribution density of formed particles around the printed area as shown in Fig. 7(d, e). The fracture surfaces of samples with printed PMMA film also agreed with the observation as shown in Fig. 6(b). The printed PMMA thin film broke down into randomly dispersed PMMA particles with a wide range of diameters as shown in Fig. 7(f). The fracture surfaces of film printed samples showed greater roughness than that of the other groups, indicating more energy was involved in the crack propagation.

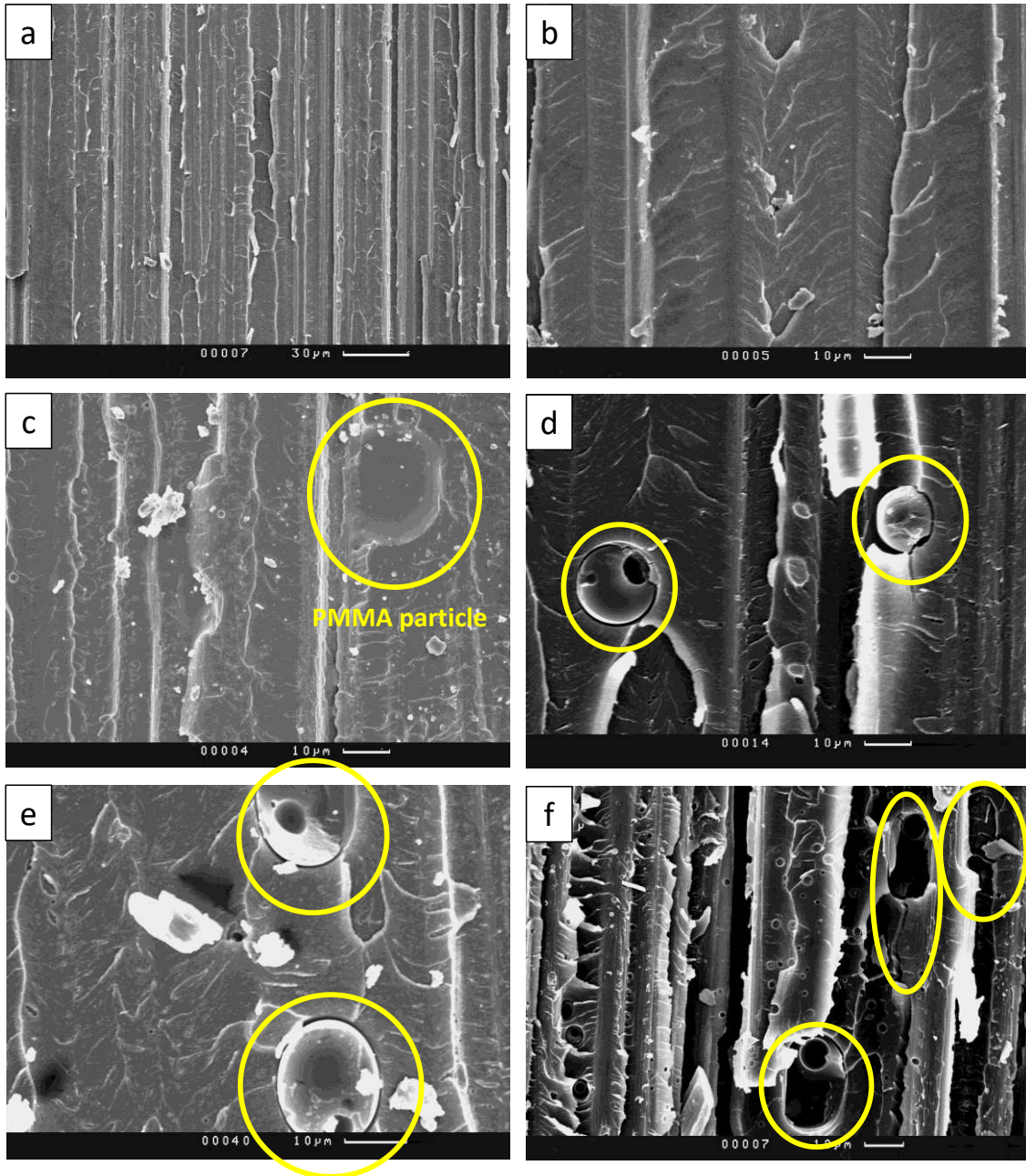


Fig. 7. Fracture surfaces of DCB tested samples showing PMMA particles formed from different printed features embedded between laminate plies. a) and b) without printed PMMA (control); c) Discrete dot pattern; d) horizontal line; e) vertical line; f) film. The circles indicate PMMA particles.

3.3 Toughening mechanisms

Epoxy toughened by thermoplastic modifiers has been reported as an effective method to overcome the drawbacks of using brittle epoxy as a composite matrix. A variety of toughening mechanisms¹⁸⁻²² have been proposed to explain the improved toughness as shown in Fig. 8. Based on the observed morphology evolution of PMMA deposits, the following two mechanisms were believed as the main reasons to explain the improved toughening of the PMMA printed systems: (1) PMMA particles act as crack stoppers which can absorb energy by plastic deformation. Given the viscoelastic nature of PMMA, the well dispersed PMMA particles provide an energy absorption path by plastic deformation, which can decelerate crack growth as the crack tips are shielded by the thermoplastic regions; (2) Debonding between PMMA particles and their surrounding epoxy resin matrix due to the limited compatibility of PMMA with the epoxy resin. As can be seen from Fig. 7, PMMA particles tended to debond from the epoxy matrix, and this process is thought to increase the fracture surface area due to the deflected crack path.

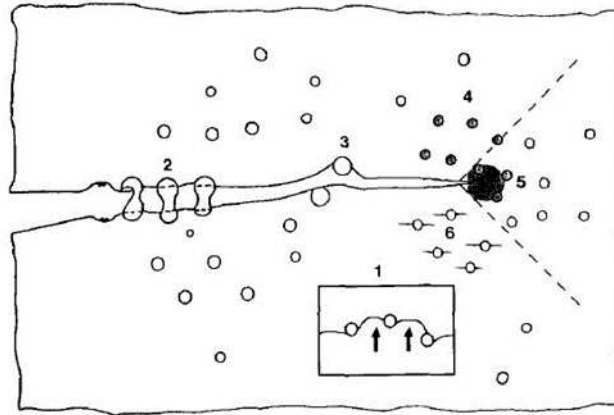


Fig. 8. Schematic showing the toughening mechanisms proposed for epoxies toughened by thermoplastic modifiers. 1) crack pinning; 2) particle bridging; 3) crack path deflection; 4) particle yielding; 5) particle yielding induced shear banding and 6) microcracking²².

3.4 Mechanical test results

3.4.1 Effect of pattern variation on G_{Ic}

It can be seen in Fig. 9 that all systems with printed PMMA deposits had improved G_{Ic} with values ranging from 15% to 41% compared to the non-printed (NP) control as expected. As mentioned in section 2.3, the four different patterns have the same material usage per unit area which is calculated as approximately 0.03 wt.%. Particularly, the system with the printed hexagonal dot pattern possessed the highest improved G_{Ic} corresponding to the crack initiation (NL: non-linear point) and propagation (PROP) among the other systems. The G_{Ic} improvements for NL and PROP compared to NP were

30% and 40% respectively. In order to check the statistical significance of these results the difference in means between the different groups was tested using one-way analysis of variance (ANOVA). The results of the ANOVA show that the means of the NL points [$F(4,20) = 6.29, p = 0.0019$] and PROP points [$F(4,20) = 17.43, p = 2.66 \times 10^{-6}$] are not equivalent as the p values are all smaller than the significance level ($\text{Alpha} = 0.05$).

The differences in size and geometry distribution of formed PMMA particles on the fracture surfaces are offered as explanation. Although the four patterns had the same amount of PMMA per unit area deposited between mid-plyes, the distribution of PMMA particles in the systems with printed lines was not as even as that of the systems with printed discrete dots in terms of size and geometry as can be seen in Fig. 6. The rectangle dot pattern provided evenly dispersed PMMA particles, however it is thought that these dots are distributed in too regular a fashion to deflect the crack path corresponding to a relatively lower G_{Ic} improvement compared to the hexagonal dot pattern. Therefore, it is assumed that the hexagonal dot pattern provides more complex crack paths for crack propagation which corresponds to a higher fracture toughness, resulting in an optimum ratio between crack deflection capability and the minimum disruption to the laminate adhesion.

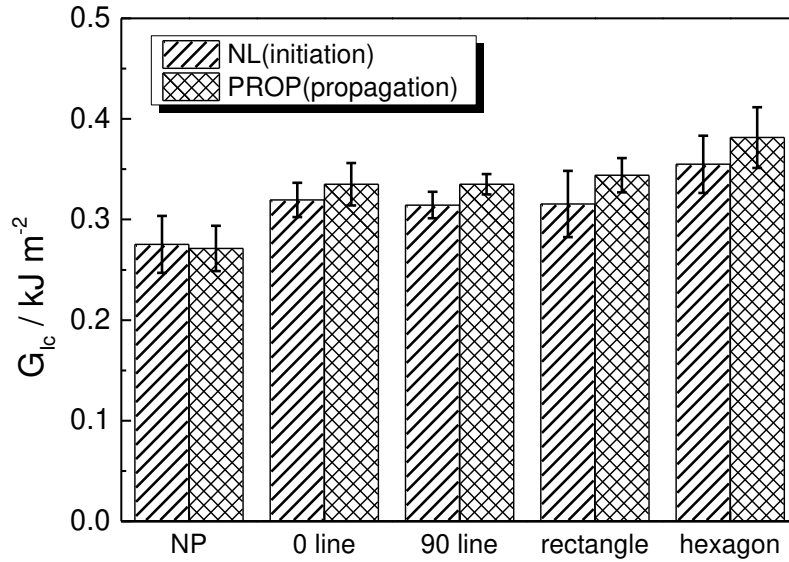


Fig. 9. G_{Ic} (initiation-NL and propagation-PROP) comparisons between samples printed with different patterns using the same amount of PMMA which is ~ 0.03 wt.%.

In order to investigate the effect of printed thin film between laminate plies on the G_{Ic} , a layer of PMMA film was printed by overlapping PMMA droplets on prepreg. Fig. 10 shows that G_{Ic} (propagation) values of the printed PMMA film system were higher than those of the systems with printed hexagonal PMMA dots and the non-printed control (NP). Statistically, the G_{Ic} (propagation) of PMMA film printed group is about 17% and 58% higher than that of hexagonal print and NP groups respectively. The result of a one-way ANOVA shows that the means of PROP points [$F(2,12) = 25.31, p = 4.95 \times 10^{-5}$] are not equivalent as the p value is significantly smaller than the significance level (Alpha =

0.05). However, PMMA usage was eight times as much as that of the discrete dot pattern system in order to achieve 100% surface coverage of PMMA on the printed surface, the percentage of PMMA weight increase is calculated as approximately 0.24 wt.%. Although the improvement in G_{Ic} of the film printed system was higher than that of the discrete dot printed CFRP, the toughening efficiency was not as high as the increase in material usage. Moreover, the standard deviations of G_{Ic} of the film printed system was dramatically higher than that of the other systems, indicating the inhomogeneity of the distribution of PMMA and the lack of adhesion between epoxy zones in the adjacent plies. This resulted in the unstable crack propagation and reduced engineering design predictability in PMMA film printed samples as shown in Fig. 11.

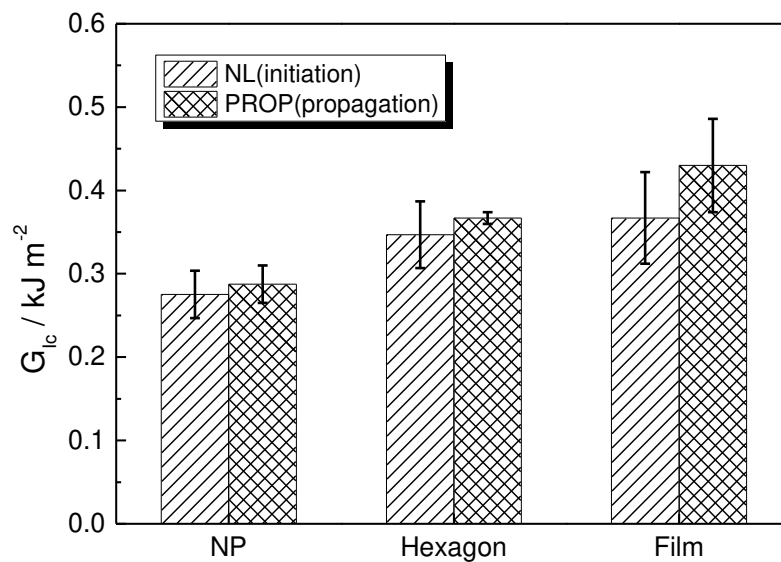


Fig. 10. G_{Ic} (initiation-NL and propagation-PROP) comparisons between samples printed with different patterns* .

**: the DCB results of NP and Hexagon are different from Fig. 9 due to the repair of autoclave which was used to cure the composite panels. In order to exclude any possible effect of new autoclave on the final panels, additional groups of the NP and hexagon have used in this experiment.*

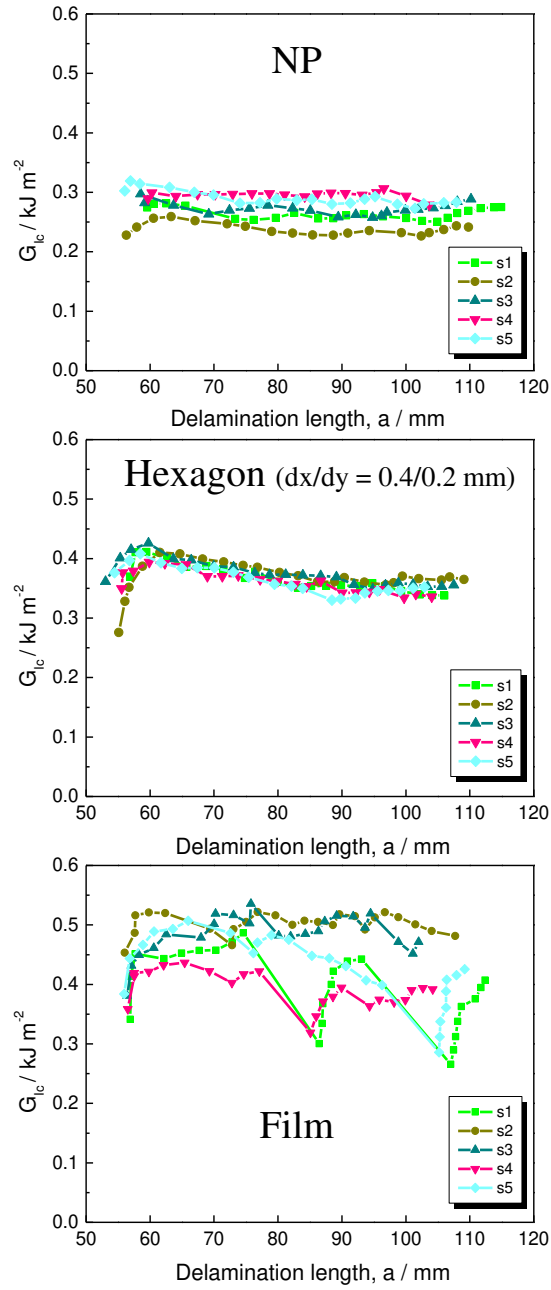


Fig. 11. The stability comparison of crack propagation between samples without/with printed discrete dot pattern and film.

3.4.2 Crack interaction with toughened and untoughened regions

Fig. 12 shows the DCB test results of the selectively patterned systems. It is clearly observed that the PMMA printed part within both systems had a higher G_{Ic} than that of the non-printed part. Fig. 12(b) shows the average G_{Ic} values of both partially printed systems (A and B): the printed part had an approximately 15% increase in G_{Ic} compared to that of the non-printed part. This result indicated that the selective printing was feasible with inkjet printing, as the printing pattern could be pre-designed via computer, and complex patterns could be easily obtained. Therefore, if the stress concentration points can be identified from a structure, these areas can be selectively printed with different or more toughening materials.

Another advantage of the selective toughening is that the cure process of the original resin system can still be preserved without excessive interruption, therefore, the resin matrix still possesses good mechanical properties, and the negative effect of the introduced toughening material on the mechanical performance can be reduced to a minimum.

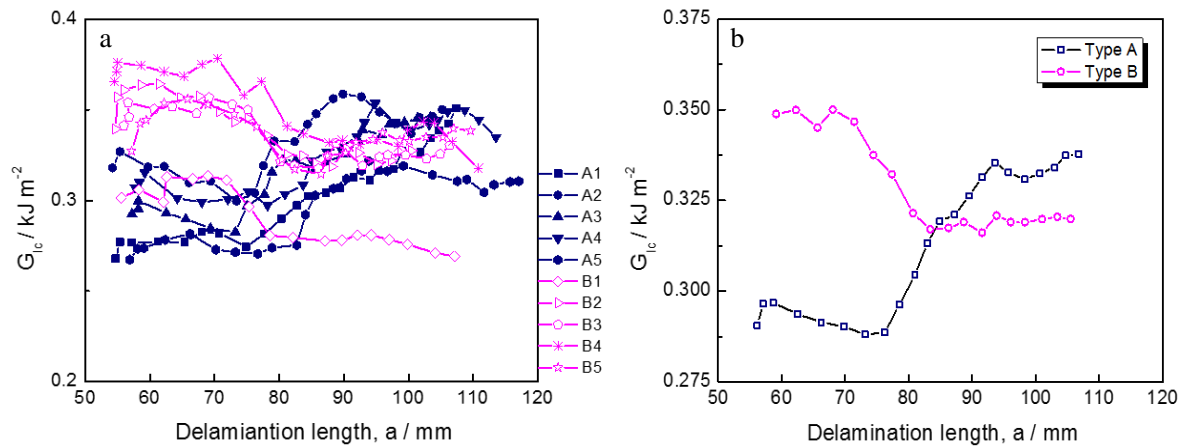


Fig. 12. The comparison of G_{Ic} between printed zone to non-printed zone. a) individual G_{Ic} -Delamination curve for each sample; b) the average G_{Ic} of group A and B ($n = 5$).

4. Conclusions

PMMA deposits, in form of printed patterns of discrete dots and continuous patterns such as lines and films, deposited by inkjet printing, tend to form spherical particles after a heating cycle on epoxy resin. The G_{Ic} (PROP) of PMMA printed, i.e. hexagon discrete dot pattern and film, CFRP laminates can be improved by 41% and 58% respectively. However, the toughening material/PMMA usage in the two systems is only ~ 0.03 wt.% and ~ 0.24 wt.% respectively. The controllability of PMMA particles formation in terms of their size and geometry distribution in discrete dot-printed systems was better compared to that of continuous patterns. Based on the observation of morphology evolution of PMMA deposits and fractographic analysis of DCB tested fracture surfaces,

the following two failure mechanisms were believed to yield the improvement in G_{Ic} : (1) PMMA particles act as crack resistance by absorbing energy through plastic deformation; (2) debonding and crack deflection between PMMA particles and their surrounding epoxy matrix increases the energy needed to propagate cracks. It has been shown that the inkjet printing technique (representing all similar printing techniques) can be used to selectively deposit toughening material to achieve selective toughening. By doing this, structures with identified stress concentration points can be selectively toughened, without incurring any parasitic weight.

Acknowledgements

The research reported in this paper was sponsored initially by the Air Force Office of Scientific Research, Air Force Material Command, USAF, under grant numbers FA8655-11-1-3072 and FA8655-13-1-3090 then by the US Army under grant number W911NF-14-1-0581. The U.S. Government is authorised to reproduce and distribute reprints for Governmental purpose notwithstanding any copyright notation thereon. The authors wish to acknowledge colleagues from the European Office of Aerospace Research and Development (a detachment of the Air Force Office of Scientific Research) for their guidance and support. In particular, we wish to thank Dr Lee Byung (Les), Dr Randall Pollak (Ty), Mr John Preston and Dr Matthew Snyder for their strong support of our research. The authors also wish to thank the Department of Mechanical Engineering,

University of Sheffield for their financial support connected to the lab class inkjet printer, and the US Army for continuing to finance and to patent our ongoing research. We also acknowledge strong support from the Knowledge Transfer Network in promoting this research and in particular Dr Steve Morris (KTN), Dr Fred Dobson (The University of Sheffield's KTP Office) and Dr Elliot Fleet from Netcomposites.

References

1. Diamanti K and Soutis C. Structural health monitoring techniques for aircraft composite structures. *Progress in Aerospace Sciences*. 2010; 46: 342-52.
2. Arai M, Noro Y, Sugimoto K-i and Endo M. Mode I and mode II interlaminar fracture toughness of CFRP laminates toughened by carbon nanofiber interlayer. *Composites Science and Technology*. 2008; 68: 516-25.
3. Pearson RA and Yee AF. Toughening mechanisms in thermoplastic-modified epoxies: 1. Modification using poly (phenylene oxide). *Polymer*. 1993; 34: 3658-70.
4. Wang CH, Sidhu K, Yang T, Zhang J and Shanks R. Interlayer self-healing and toughening of carbon fibre/epoxy composites using copolymer films. *Composites Part A: Applied Science and Manufacturing*. 2012; 43: 512-8.
5. Hojo M, Ando T, Tanaka M, Adachi T, Ochiai S and Endo Y. Modes I and II interlaminar fracture toughness and fatigue delamination of CF/epoxy laminates with self-same epoxy interleaf. *International Journal of Fatigue*. 2006; 28: 1154-65.

6. Khan SU and Kim J-K. Improved interlaminar shear properties of multiscale carbon fiber composites with bucky paper interleaves made from carbon nanofibers. *Carbon*. 2012; 50: 5265-77.
7. Zeng Y, Liu H-Y, Mai Y-W and Du X-S. Improving interlaminar fracture toughness of carbon fibre/epoxy laminates by incorporation of nano-particles. *Composites Part B: Engineering*. 2012; 43: 90-4.
8. Meier H, Löffelmann U, Mager D, Smith PJ and Korvink JG. Inkjet printed, conductive, 25 µm wide silver tracks on unstructured polyimide. *physica status solidi (a)*. 2009; 206: 1626-30.
9. Park BK, Kim D, Jeong S, Moon J and Kim JS. Direct writing of copper conductive patterns by ink-jet printing. *Thin Solid Films*. 2007; 515: 7706-11.
10. Tekin E, Smith PJ, Hoepfener S, et al. Inkjet printing of luminescent CdTe nanocrystal-polymer composites. *Advanced Functional Materials*. 2007; 17.
11. Zhang Y, Stringer J, Grainger R, Smith PJ and Hodzic A. Improvements in carbon fibre reinforced composites by inkjet printing of thermoplastic polymer patterns. *physica status solidi (RRL) – Rapid Research Letters*. 2014; 8: 56-60.
12. Zhang Y, Stringer J, Grainger R, Smith PJ and Hodzic A. Fabrication of patterned thermoplastic microphases between composite plies by inkjet printing. *Journal of Composite Materials*. 2014: 0021998314533715.

13. Zhang Y, Stringer J, Smith P, Hodzic A and Grainger R. Toughening composites with self-ameliorating capability using inkjet printing technique. *16th European Conference On Composite Materials*. Seville, Spain 2014.
14. Fleet EJ, Zhang Y, Hayes SA and Smith PJ. Inkjet printing of self-healing polymers for enhanced composite interlaminar properties. *Journal of Materials Chemistry A*. 2015; 3: 2283-93.
15. Fibre-reinforced plastic composites. Determination of mode I interlaminar fracture toughness. BSI, 2002.
16. Gomez CM and Bucknall CB. Blends of poly (methyl methacrylate) with epoxy resin and an aliphatic amine hardener. *Polymer*. 1993; 34: 2111-7.
17. Ritzenthaler S, Girard-Reydet E and Pascault J. Influence of epoxy hardener on miscibility of blends of poly (methyl methacrylate) and epoxy networks. *Polymer*. 2000; 41: 6375-86.
18. Maxwell D, Young RJ and Kinloch AJ. Hybrid particulate-filled epoxy-polymers. *Journal of Materials Science Letters*. 1984; 3: 9-12.
19. Bucknall CB and Gilbert AH. Toughening tetrafunctional epoxy resins using polyetherimide. *Polymer*. 1989; 30: 213-7.
20. Pearson RA and Yee AF. Influence of particle size and particle size distribution on toughening mechanisms in rubber-modified epoxies. *Journal of Materials Science*. 1991; 26: 3828-44.

21. Riew CK and Kinloch AJ. Toughened plastics I: science and engineering. American Chemical Society, Washington, DC (United States), 1993.
22. Pearson RA and Yee AF. Toughening mechanisms in elastomer-modified epoxies. *Journal of Materials Science*. 1989; 24: 2571-80.